The Constructal Evolution of the Cross Sections of Jets Toward the Round Shape

by

Shiva Ziaei

Department of Mechanical Engineering and Materials Science
Duke University

Date:_____

Approved:

_____

Adrian Bejan, Co-Supervisor

_____

Sylvie Lorente, Co-Supervisor

_____

Edward J. Shaughnessy

Thesis submitted in partial fulfillment of
the requirements for the degree of
Master of Science in the Department of
Mechanical Engineering and Materials Science in the Graduate School
of Duke University
2013

ABSTRACT

The Constructal Evolution of the Cross Sections of Jets Toward the Round Shape

by

Shiva Ziaei

Department of Mechanical Engineering and Material Science
Duke University

Date:_____

Approved:

_____

Adrian Bejan, Co-Supervisor

_____

Sylvie Lorente, Co-Supervisor

_____

Edward J. Shaughnessy

An abstract of a thesis submitted in partial
fulfillment of the requirements for the degree
of Master of Science in the Department of
Mechanical Engineering and Materials Science in the Graduate School of
Duke University
2013

Abstract

This thesis reports a theoretical and experimental study of laminar and turbulent jet flows issuing from a slender rectangular nozzle. According to constructal law of design and evolution in nature, all flow systems have a tendency to evolve into configurations that facilitate flow access over time. Therefore this law predicts that when a jet initially has a flat cross-section, further downstream it would evolve toward round cross-sections for the purpose of enhancing the transfer of momentum (movement) perpendicular to the jet, i.e. to enhance mixing. The first part of the study consists of numerical simulations conducted in range of Re = 10, 20 and 30 for laminar jet flow, and Re = 500, 1000, 2000, 5000 and 10000 for turbulent jet flow, where Re is the Reynolds number based on nozzle spacing and velocity. In the second part, the phenomenon is studied based on scale analysis. The chief conclusions of this part is that the prediction of the transition from flat to round cross-section is in agreement with the results produced by numerical experiments. The experimental observations of jet flows are in accordance with the constructal law.

Contents

List of Tables

List of Figures

Nomenclature

A	Cross sectional area of contours of constant longitudinal velocity [m^2]
D	Diameter of cylindrical domain [m]
D_h	Hydraulic diameter [m]
I	Turbulent intensity
κ	Kinetic energy of turbulence [m^2/s^2]
L	Width of rectangular nozzle [m]
p	Perimeter of contours of constant longitudinal velocity in the cross section [m]
u_j	Velocity vector in the j th direction [m/s]
U_0	Uniform nozzle velocity [m/s]
W	Spacing of rectangular nozzle [m]
x	Distance from nozzle in the downstream direction [m]
ε	Dissipation of turbulent kinetic energy [m^2/s^3]
μ	Dynamic viscosity [Pa.s]
ν_t	Turbulent viscosity [m^2/s]
ν	Kinematic viscosity [m^2/s]
ρ	Density [kg / m^3]

Acknowledgements

There are no proper words to convey my deep gratitude and respect for my thesis advisor, Prof. Adrian Bejan. His insightful comments and constructive criticisms at different stages of my research were thought-provoking and they helped me focus my ideas. I am grateful to him for holding me to a high research standard and enforcing strict validations for each research result, and thus teaching me how to do research. I consider it an honor to work with him. One simply could not wish for a better or friendlier supervisor.

My sincere thanks must also go to my co-advisor Prof. Sylvie Lorente. She generously gave her time to offer me valuable comments toward improving my work. I deeply acknowledge her support and help. Working with her is a great experience that I will cherish forever.

I would like to thank Prof. Edward Shaughnessy for taking time out from his busy schedule to serve as my committee member at my thesis defense.

Last but not least, I would like to express my heart-felt gratitude to my family for their unconditional trust, timely encouragement, and endless patience for which my mere expression of thanks likewise does not suffice.

1. Introduction

Throughout nature, flow systems exhibit the tendency to morph freely into configurations that flow more easily and for greater access. For example, flows that connect areas with points, and volumes with points, evolve into tree-shaped flow architectures with seemingly precise rules of construction, robustness and persistence. This happens throughout animate systems (vascular tissues, lungs) and inanimate systems (river basins and deltas, lightning).

This natural tendency is now recognized as the phenomenon of design in nature: the occurrence of design (organization), its rules of construction, and its evolution over time. This phenomenon is covered by the constructal law, which states that: "For a finite-size flow system to persist in time (to live), its configuration must evolve in such a way that provides greater and greater access to the currents that flow through it [1]."

A distinct group of design-in-nature phenomena consists of even simpler flow configurations that unite the animate with the inanimate flow systems. They are the cross-sectional shapes of the channels and ducts through which natural streams flow. Without exception, the cross sections tend to the round: blood vessels, pulmonary airways, underground rivers, large pores in the hill slope, underground galleries of moles and earthworms, intestines and other flow ducts in animal design [2]. When the cross-sections have a free surface, as in river channels, the natural tendency to evolve toward the round cross-section is visible in the proportionality between depth and width in rivers of all sizes [1-3].

In this thesis, we focus on an even simpler phenomenon of evolution toward the round cross section: jets and plumes that start originally as flat sheets, and eventually develop round cross sections. We will see that this tendency is present in both laminar and turbulent flow. This phenomenon is simpler than in the preceding paragraph because jets and plumes are fluid streams that penetrate (i.e., flow through) bodies of the same fluid as the stream. In the examples of the preceding paragraph, every stream flows through a solid duct, which is relatively free to morph.

Turbulent free jets issuing from noncircular slots or nozzles are used extensively in technical areas of interest ranging from aerospace to chemical to mechanical engineering, such as aircraft design, gas turbine combustors, and cooling systems for turbine blades. Several studies have been devoted to free jets issuing from circular and noncircular nozzles, which investigated the effect of the shape and size of the nozzle on jet development [4-6].

Previous studies measured velocity and temperature fields using linearized hot-wire anemometers [7-10]. There are three regions in the downstream direction of a three-dimensional jet. The first is the potential core region. This region contains the flow close to the jet exit with uniform longitudinal velocity, because mixing at the jet edges has not yet spread across the jet. Next is a region with decreasing longitudinal velocity that is dependent on nozzle configuration. This region bears the influence of the initial geometry of nozzle. Further downstream is an axisymmetric decay region, which contains axisymmetric flow that is independent of nozzle configuration. The velocity

profile is similar in both symmetry planes of the nozzle. Even farther downstream, a fourth regime of fully axisymmetric flow is observed [11-18].

Beginning with chapter 2, in which the laminar and turbulent flows are simulated numerically, we show that sufficiently far downstream the flat cross section of the jet or plume is replaced by a round cross section. We also show that this evolutionary change is in accord with the constructal law. Finally, we show that the downstream locations of the transitions to round cross sections can be predicted theoretically.

2. Numerical experiments

In this chapter, numerical simulations of jets are described so that the data can be compared with the results predicted from the theory of chapter 5. The computational domain and boundary conditions used in the simulation of laminar and turbulent jets are shown in Figurs 2.1. The jet of fluid issuing from the rectangular nozzle enters the flow field, which is modeled as cylindrical domain with the diameter D, where D = 4L. We found that the size of the domain is large enough so that it does not affect the numerical results. For simplicity, the lateral boundary of the domain was first modeled as an impermeable wall, and the no slip condition was specified on it for laminar and turbulent jet flow. Later, the lateral boundary condition was changed to zero shear. The velocity through the jet nozzle exit is uniform and specified. The aspect ratio of slit nozzle is L/W= 10.

The distance from the slit nozzle in streamwise direction is x. The outlet pressure condition is imposed on the outlet plane of the flow domain. Because both jets and plumes flow into a surrounding fluid reservoir, uniform pressure and radially invariant pressure are applied as boundary conditions.

The Reynolds numbers for which simulations have been performed are 10, 20 and 30 for laminar flow and 500, 1000, 2000, 5000 and 10000 for turbulent flow. The commercial CFD software ANSYS and FLUENT was used to simulate the laminar jets and turbulent jets.

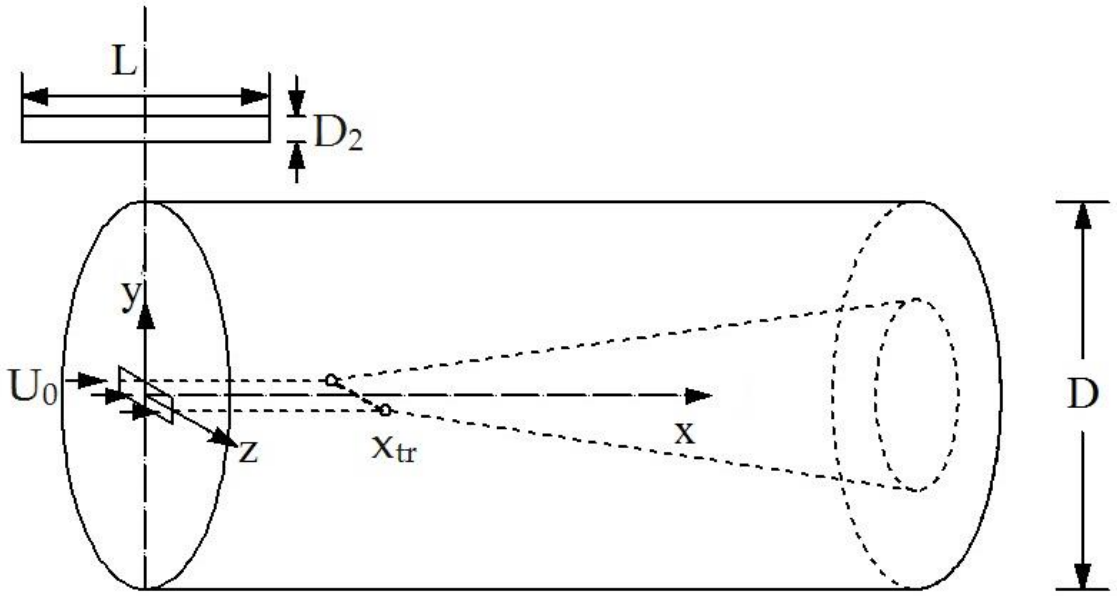

Figure 2.1: The computational flow domain for simulation of laminar and turbulent jets.

The mathematical model used in this work is based on the Navier-Stokes system of differential equations with the Reynolds method of averaging the time-dependent equations. For the turbulent jet simulation, the RNG κ-ε model was utilized. This model is derived from the instantaneous Navier-Stokes equations, using the mathematical technique called "renormalization group" (RNG) method. This model is similar to standard κ-ε model with different constants and additional terms and functions in the transport equations. The κ-ε model has become one of the most widely used turbulence models as it provides robustness, economy and reasonable accuracy for a wide range of turbulent flows. The Navier-Stokes method using the standard κ-ε turbulence model is capable of predicting the transition behavior of

turbulent plumes properly, while such predictions are made without any modification to the published constants for the turbulence model. Assuming appropriate treatment of the near wall region, the RNG model uses an analytically derived differential formula for the effective turbulent viscosity which accounts for low Reynolds number flows. The RNG κ-ε model is therefore more accurate and more reliable than the standard κ-ε model for a wider range of flows.

The Reynolds numbers are calculated from equation (2-1) where W, U_0, and ν denote for the nozzle spacing, nozzle exit velocity and kinematic viscosity of air at 50 °C, namely 1.7894×10^{-5} m^2/s, respectively,

$$Re = \frac{U_0 W}{\nu} \qquad (2.1)$$

The time-averaged, governing equations for incompressible turbulent flow are expressed as follows:

Conservation of mass:

$$\frac{\partial \overline{u}_j}{\partial x_j} = 0 \qquad (2.2)$$

Where $\bar{u}_j$ is the mean velocity vector in the j th direction.

Conservation of momentum:

$$\bar{u}_j \frac{\partial \bar{u}_i}{\partial x_j} - \frac{\partial}{\partial x_j}\left[(\nu_t + \nu) \left(\frac{\partial \bar{u}_i}{\partial x_j} + \frac{\partial \bar{u}_j}{\partial x_i} \right) \right] = -\frac{\partial p}{\partial x_i} \qquad (2.3)$$

where ν is the kinematic viscosity and ν_t is the turbulent viscosity given by:

$$\nu_t = C_\mu \frac{\kappa^2}{\varepsilon} \qquad (2.4)$$

where C_μ = 0.0845 is a constant, κ is the kinetic energy of turbulence, and ε is dissipation of turbulent kinetic energy

Two additional conditions are the equations for the conservation of kinetic energy of turbulence κ and its dissipation ε:

Conservation of turbulent kinetic energy for incompressible flow field:

Conservation of dissipation of turbulent kinetic energy for incompressible flow field:

$$\frac{\partial \varepsilon}{\partial t} + \bar{u}_j \frac{\partial \varepsilon}{\partial x_i} = \frac{\partial}{\partial x_j}\left(\frac{\nu_t}{\sigma_\varepsilon} \frac{\partial \varepsilon}{\partial x_j} \right) \frac{\partial}{\partial x_j} \frac{\partial u_i}{\partial x_j} + C_{\varepsilon 1} \frac{\varepsilon}{\kappa} \nu_t \left(\frac{\partial \bar{u}_i}{\partial x_j} + \frac{\partial \bar{u}_j}{\partial x_i} \right) \frac{\partial \bar{u}_i}{\partial x_j} - C_{\varepsilon 2} + \rho g_i \qquad (2.6)$$

Standard values of the model constants of κ – ε turbulence model used in the model equations are [19]:

$$C_{\varepsilon 1} = 1.42 \ , \ C_{\varepsilon 2} = 1.92 \ , \ \sigma_k = 1.0 \ , \ \sigma_\varepsilon = 1.3$$

Equations (2.7) and (2.8) are used for boundary conditions of turbulent simulation:

Turbulent intensity:

$$I = 0.16\,\mathrm{Re}^{-1/8} \qquad (2.7)$$

Hydraulic diameter:

$$D_h = \frac{4A}{p} \qquad (2.8)$$

Details of laminar and turbulent jets are listed in Tables 1-2, respectively.

Table 1: Numerical parameters for laminar jet simulations.

Re	Grid number	Inlet velocity (m/s)
10	312071	0.000895
20	312071	0.00179
30	312071	0.00268

Table 2: Numerical parameters for turbulent jet simulations.

Re	Grid number	Inlet velocity (m/s)	Turbulent intensity	Hydraulic diameter	backflow turbulent intensity	Backflow hydraulic diameter
500	273304	0.044735	5.5	0.364	1.2	8
1000	273304	0.08947	5.5	0.364	1.2	10
2000	273304	0.17894	5.5	0.364	1.2	12
5000	273304	0.44735	5.5	0.364	1.2	15
10000	273304	0.8947	5.5	0.364	1.2	20

3. Laminar jets

In the present numerical study, the laminar and turbulent jet simulations are grid independent and the meshing scheme is hexahedron which has the highest accuracy among the other patterns. Tables 3-6 show the transition lengths obtained from different grid-number simulations for both laminar and turbulent flows.

Table 3: Transition lengths of Re = 10 for different grid number.

Grid Number	x_{tr}/L
312071	1.6
285780	1.7
190520	2.1

Table 4: Transition lengths of Re = 20 for different grid number.

Grid Number	x_{tr}/L
312071	3
285780	3.05
190520	3.3

Table 5: Transition lengths of Re = 30 for different grid number.

Grid Number	x_{tr}/L
312071	4.8
285780	4.9
190520	5.75

Table 6: Transition lengths of turbulent jet flow for different grid number.

Grid Number	x_{tr}/L
273304	10
250278	10.5
166852	11.2

We begin with the case of laminar jets at the Reynolds numbers 10, 20 and 30. For all of these cases, the cross sectional area of the simulated jet evolved from the slot nozzle in a particular pattern, from rectangular to horizontal elliptical, circular, vertical elliptical, and circular again. Figure 3.1 demonstrates the evolution of the cross sectional area downstream from the jet nozzle, to the distance 10L.

In order to identify the transition distance where the rectangular cross sectional area changes to a round cross section, we plotted $p/A^{1/2}$ versus x/L, where p and A are the perimeter and area of contours of constant longitudinal velocity in the cross section. By convention, we selected $u = \frac{1}{2} u_c$, as the longitudinal speed that defines the contour monitored in order to document the evolution of the shape of the cross section. In this definition, u_c is the centerline velocity, as the longitudinal velocity inside the cross section. At the nozzle, the shape is flat, and $p/A^{1/2}$ is large, comparable with $2 L / (LW)^{1/2} = 2 (L / W)^{1/2} >> 1$. Downstream, $p/A^{1/2}$ is smaller, and its smallest value occurs when the contour is round. In that limit, if the radius of the contour line is r, then $P / A^{1/2} = 2\pi r / (\pi r^2)^{1/2} = 2\pi^{1/2} \cong 3$.

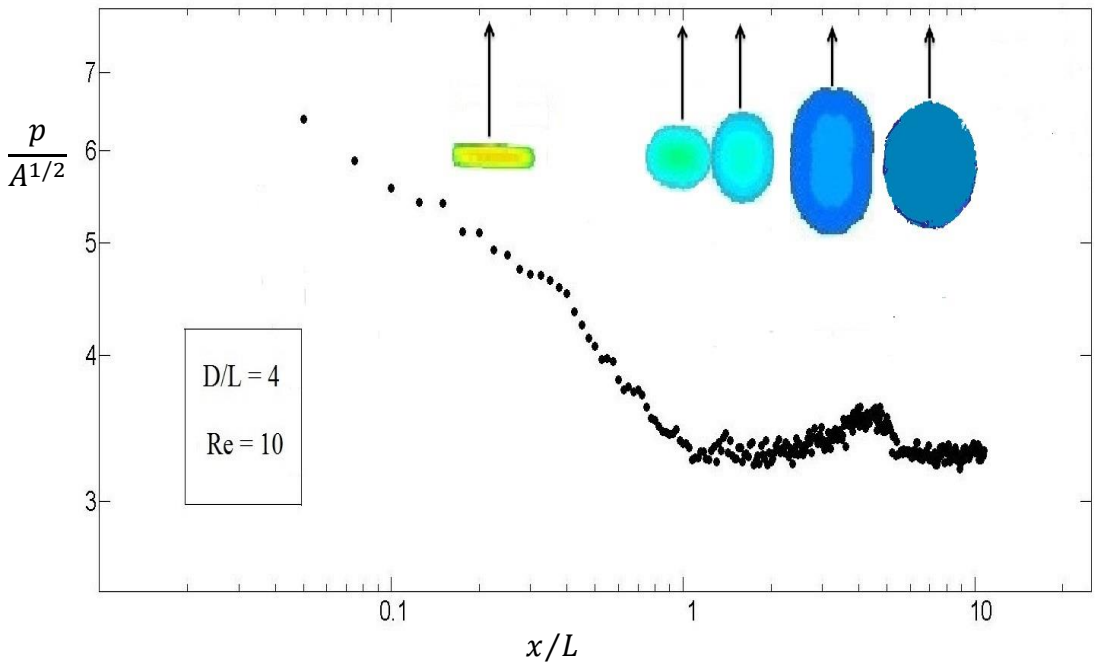

Figure 3.1: Laminar jet: evolution of streamwise constant-velocity contours for Re = 10 and the corresponding measure of the shape of the contour, $p/A^{1/2}$.

Figure 3.1 shows the evolution of cross sectional shape when Re = 10. Two changes can be observed. The first change, which is the focus of this study, occurs between x/L = 1 and x/L = 2 and displays the transition from horizontal elliptical to circular cross section. The second change takes place within x/L = 4 and x/L = 5. This change shows the transition of round jets to an elliptical cross sectional area, yet, the second ellipse is more round than the first. It can be seen from Figure 3.1 that the $p/A^{1/2}$ value reaches the value 3. This means that the flow finally evolves to the round cross section.

Figures 3.2 and 3.3 show the corresponding results for Re = 20 and Re = 30. The first change in the $p/A^{1/2}$ curve, which illustrates the conversion from horizontal ellipse to circle, is around x/L = 1.5 and x/L = 2.5 for Re = 20, and near x/L = 2 to 3 for Re = 30.

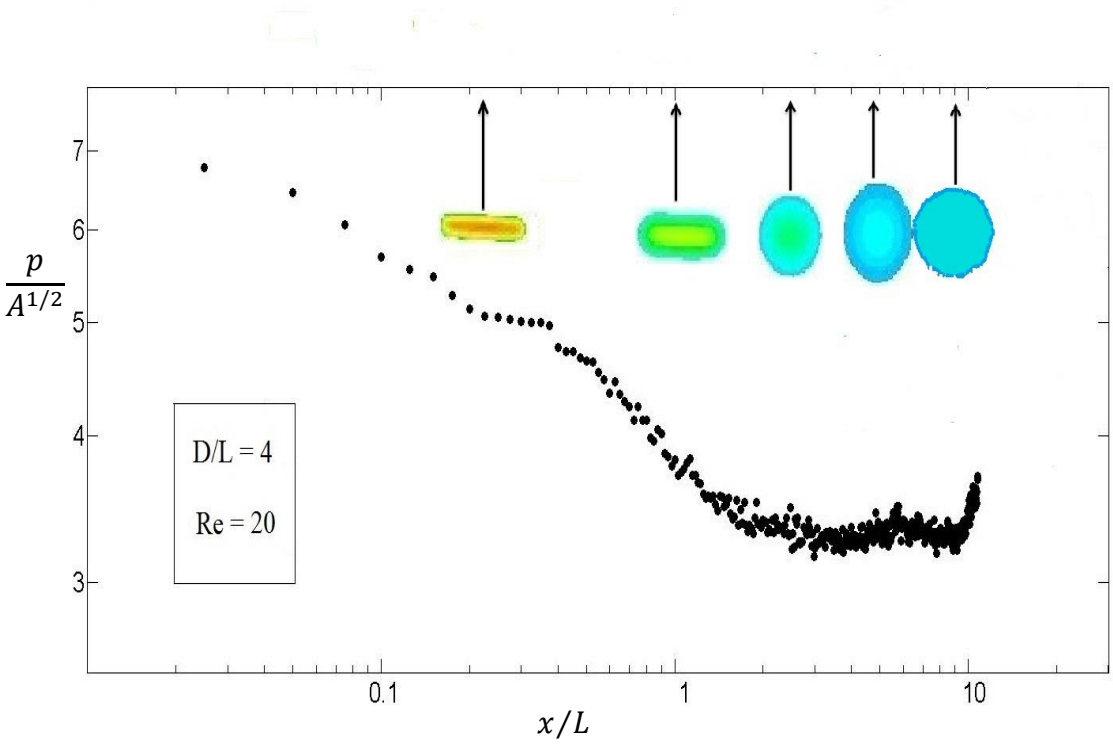

Figure 3.2: Laminar jet: evolution of streamwise constant-velocity contours for Re = 20 and the corresponding measure of the shape of the contour, $p/A^{1/2}$.

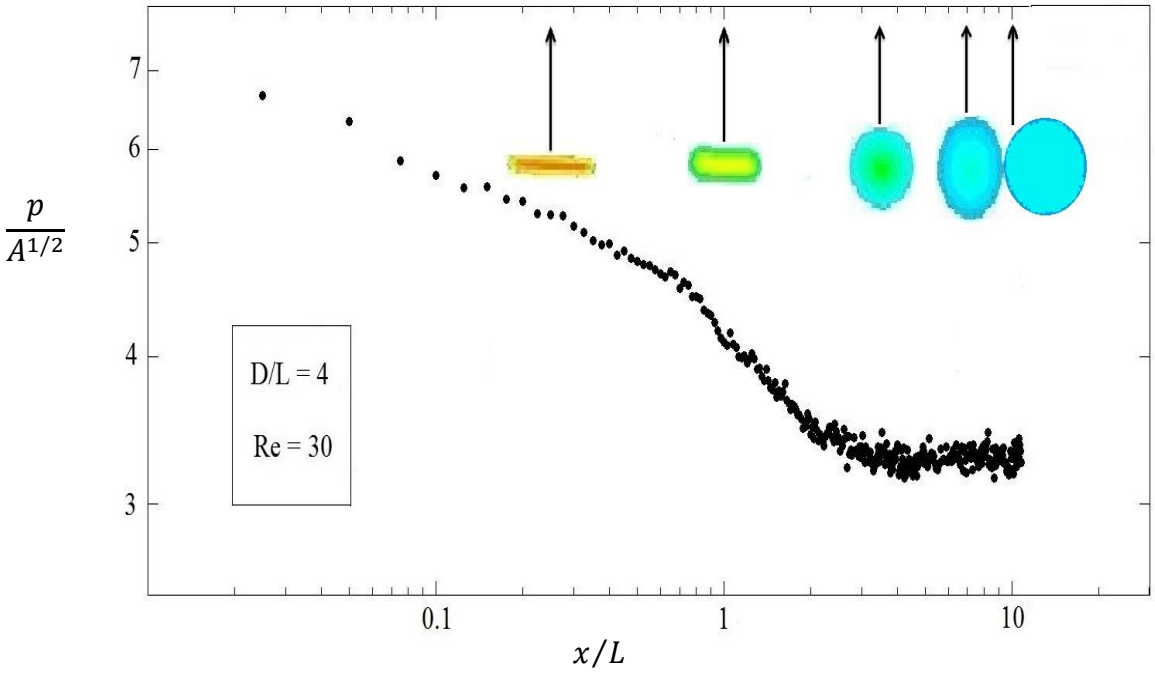

Figure 3.3: Laminar jet: evolution of streamwise constant-velocity contours for Re = 30 and the corresponding measure of the shape of the contour, $p/A^{1/2}$.

In order to compare the transition lengths of laminar jets for different Reynolds numbers, the shape plots have been plotted together in Figure 3.4. The transition occurs farther from the nozzle when the Reynolds number is larger.

These flow simulations were conducted for D/L = 4, where D is the diameter of computational domain. This D/L ratio is large enough to avoid the effect of the confining wall on the simulation of laminar and turbulent jets. This can be verified by changing the ratio D/L from 2 to 8 in increments of 2 at each simulation. Figure 3.5 shows the simulation results of Re = 10 for different D/L ratios. The curves for D/L = 4 and 8 ratios

are behaving similarly, however the D/L = 2 curve shows a significant departure from the results obtained for D/L = 4 and 8. This behavior confirms that the diameter to the width ratio of 4, which was used in this study, is large enough.

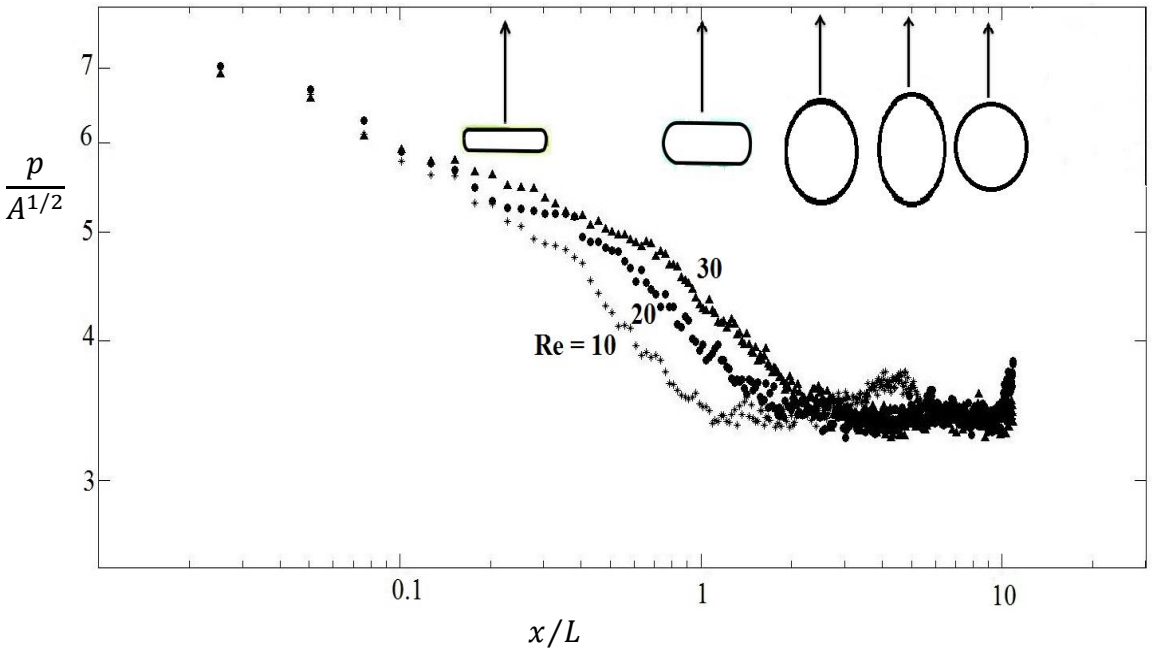

Figure 3.4: The evolution of the cross sectional shape in laminar jets at Re = 10, 20 and 30.

Simulations of spatially evolving laminar jets have been carried out in flow domains with two different shapes: cylinder and parallelepiped. These two configurations have the same nozzle velocity and boundary conditions. The different computational domain shapes were used in order to analyze the influence of domain shape on the transition to circular contours or the jets developed downstream. It can be observed from Figure 3.6 that the transitional behavior of laminar jets in parallelepipedic domains compares well with the results obtained in cylindrical domains. It is clear that

the transition distances attained from simulations do not depend on the shape of the computational domain.

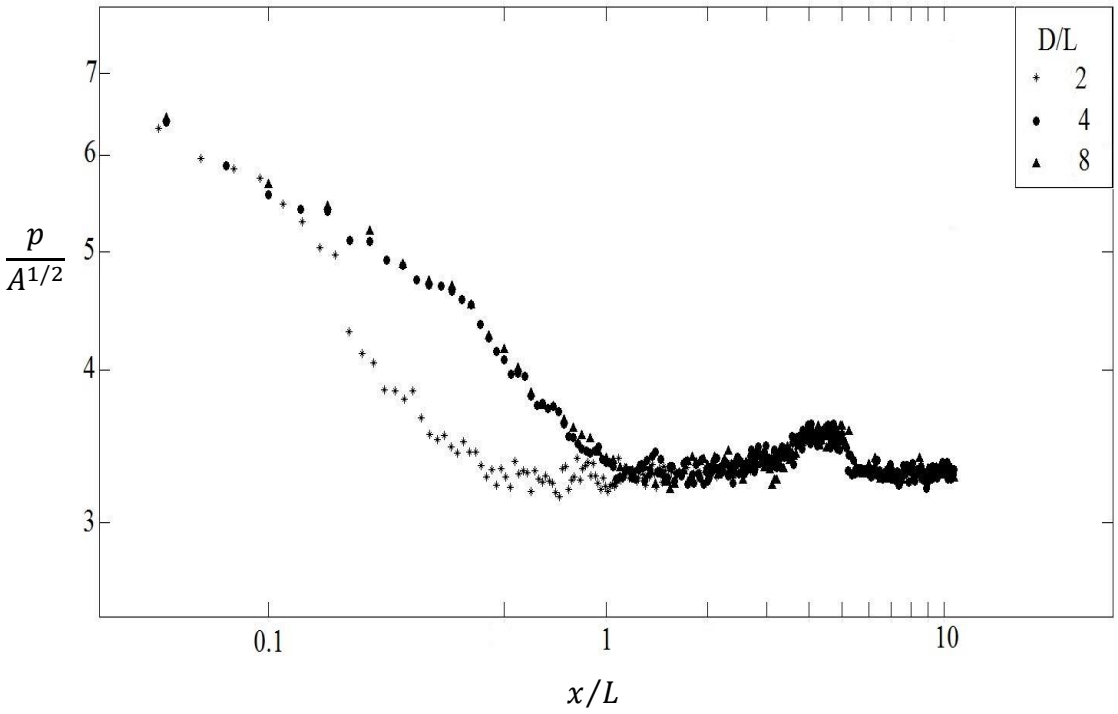

Figure 3.5: The effect of the size of the domain (D/L) on the evolution of the cross sectional shape.

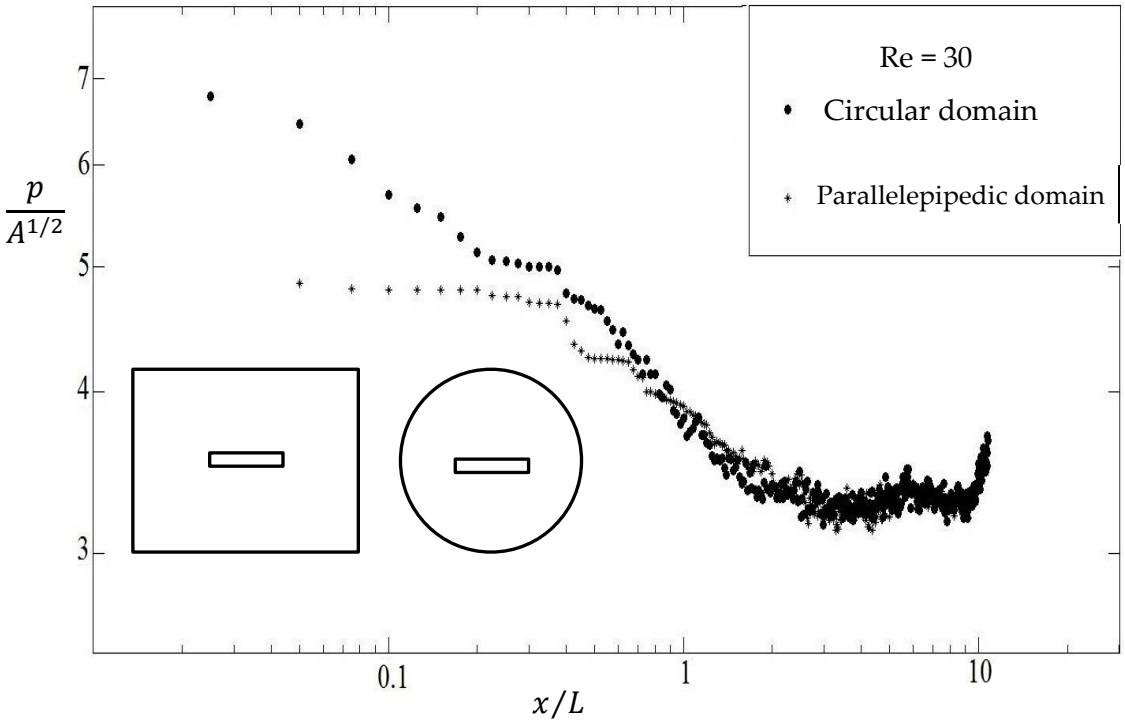

Figure 3.6: The effect of the shape of the domain cross section on the evolution of the cross sectional shape of laminar jets at Re = 30.

4. Turbulent jets

The evolution of the shape of the contour of constant longitudinal velocity for turbulent jet was investigated by simulating jet flows at Re = 500, 1000, 2000, 5000 and 10000. Figure 4.1 shows the development of streamwise contours in planes perpendicular to the jet axis. The contour starts as a rectangle and evolves into a horizontal ellipse. Farther downstream, the constant-u contour becomes a circle, and this is followed by a vertical ellipse that is considerably rounder than the first ellipse. Finally, the cross sectional shape returns to being round.

There are three changes in the contour shape evolution of Figure 4.1 which is drawn for Re = 500. The first indicates the transition from horizontal ellipse to circle, and the second shows the transition from vertical ellipse to circle. The third variation in the curve is related to the change of cross-section configuration from circle to horizontal ellipse. Note that the second elliptical configuration is much rounder than the first one. This means that the flat jet tends to acquire rounder cross-sections as it evolves farther downstream.

By performing simulations for the other Reynolds numbers associated with the turbulent flow, the changes in the contours of constant velocity exhibited the same pattern, and the transition lengths x/L were virtually invariant throughout the Re range. These results can be seen in Figure 4.2, which shows the evolution of $p/A^{1/2}$ for Re = 500, 1000, 2000, 5000 and 10000.

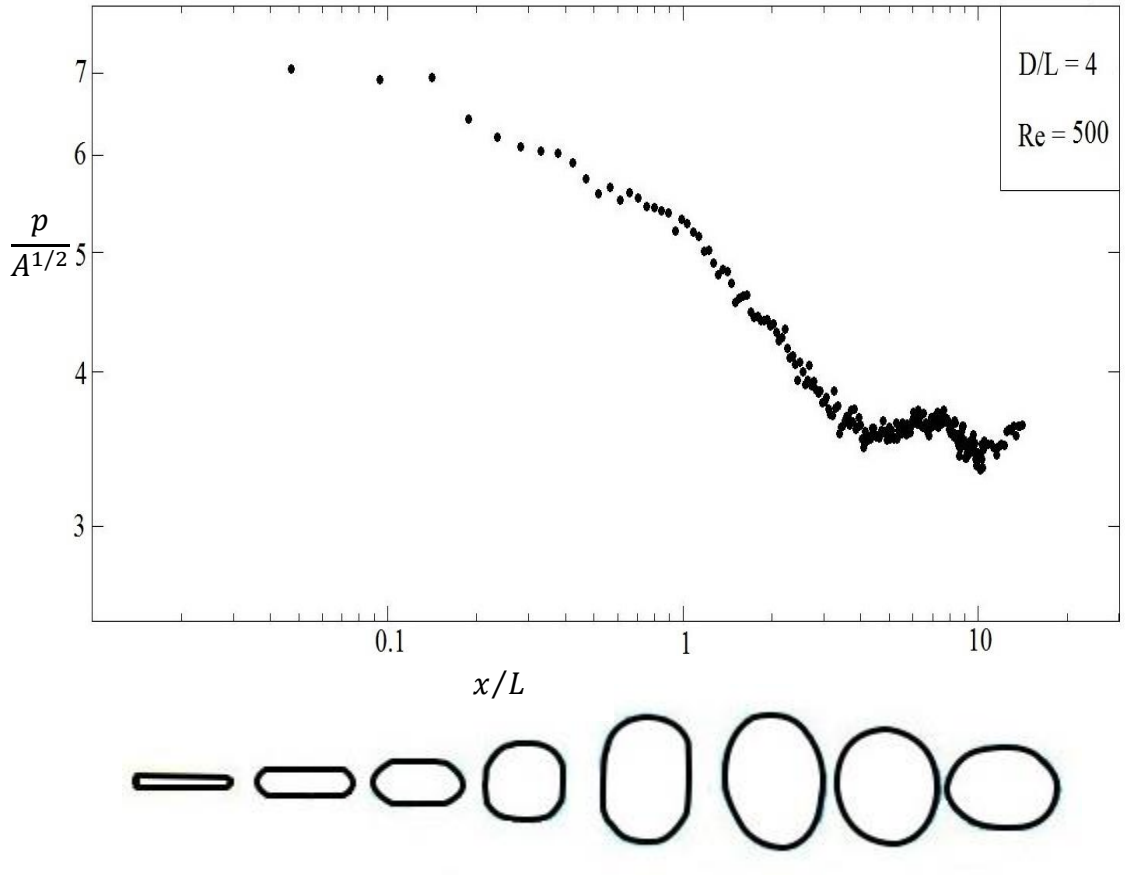

Figure 4.1: Turbulent jet: evolution of streamwise constant-velocity contours for Re = 500 and the corresponding measure of the shape of the contour, $p/A^{1/2}$.

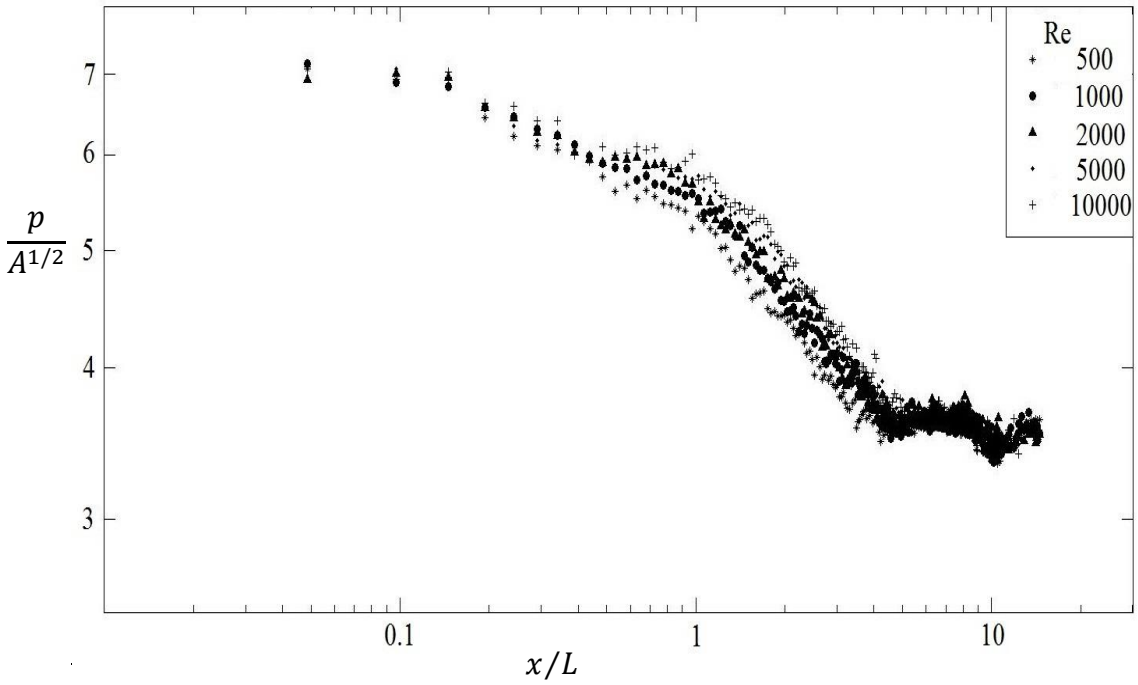

Figure 4.2: The evolution of the cross sectional shape in turbulent jets at Re = 500, 1000, 2000, 5000 and 10000.

Figure 4.3 shows the simulation results for Re = 1000 for different ratio D/L. The curves for D/L = 4 and D/L = 8 are the same, and they differ from the curve for D/L = 2. This validates the choice of D/L = 4 in this work.

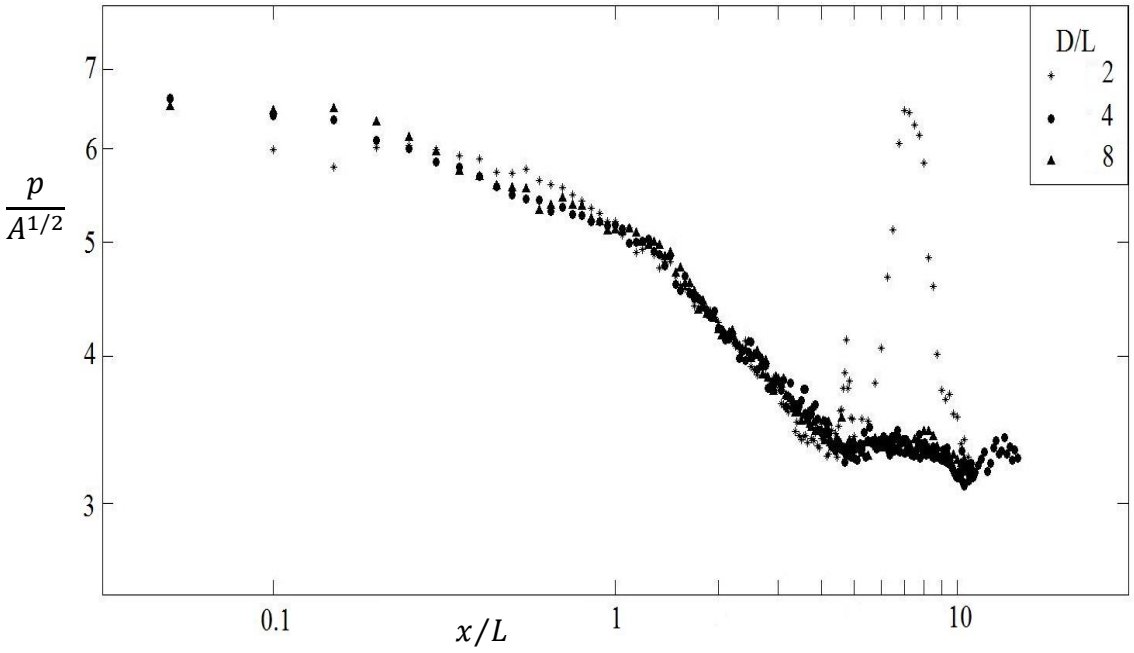

Figure 4.3: The effect of the size of the domain (D/L) on the evolution of the cross sectional shape.

In order to show that the evolution of the shape of the cross section in turbulent jets is independent of the shape of the flow domain, two turbulent flows with the same Reynolds number were simulated in parallelepipedic and cylindrical domains with the same boundary conditions. Figure 4.4 and the $p/A^{1/2}$ curve of the corresponding jets show that the transitional evolutions of turbulent flows in different domains are similar.

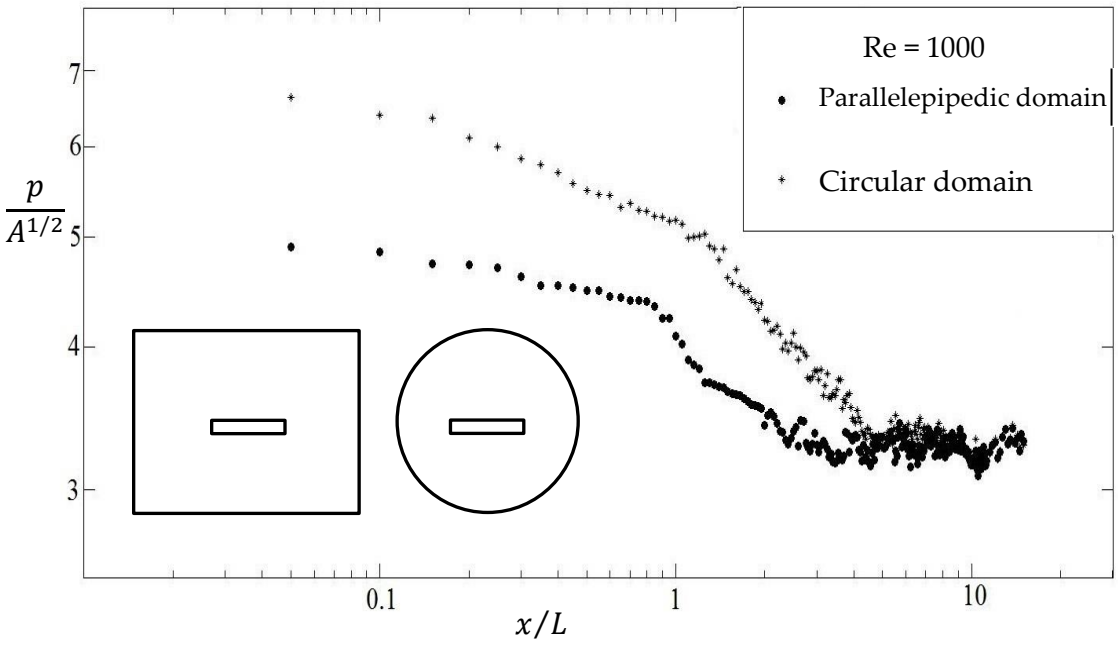

Figure 4.4: The effect of the shape of the domain cross section on the evolution of the cross sectional shape of turbulent jets at Re = 1000.

5. Comparison with the constructal law

Bejan and Lorente [20] showed that the constructal law accounts for the tendency of jets and plumes to acquire round cross sections. The reason is the natural tendency of all these flow systems to morph into configurations that facilitate the access of what flows. In jets and plumes it is the momentum that flows laterally, from the mover (the turbulent column) to the non-mover (the surroundings). We call this flow "mixing", or momentum transfer. When the lateral flow of momentum has greater access to the stationary environment, the fluid of the column mixes faster with the surrounding fluid, and its longitudinal speed decreases faster. The tendency of the flow is to morph its cross-section such that the mixing is more effective, and the longitudinal speed decreases faster.

5.1. Turbulent Jets

Consider first a two-dimensional jet issuing at speed U_0 from a slit of spacing W and width L (Figure 2.1). The scale of its longitudinal velocity decreases as $x^{-1/2}$ in the longitudinal direction [21],

$$u_2 \sim U_0 \left(\frac{3}{4} \gamma_2 \frac{D_2}{x} \right)^{1/2}, \quad (\gamma_2 = 7.67) \tag{5.1}$$

When the nozzle is round with diameter D_3 and velocity U_0, the longitudinal velocity decreases as x^{-1},

$$u_3 \sim U_0 \frac{3^{1/2}}{4} \gamma_3 \frac{D_3}{x}, \quad (\gamma_3 = 15.2) \tag{5.2}$$

This decrease is faster than in the two-dimensional jet, and it means that the round jet configuration will prevail sufficiently far downstream. The transition length (x_{tr}) beyond which the two-dimensional jet continues as a round jet is obtained by intersecting Eqs. (5.1) and (5.2),

$$x_{tr} \sim \frac{\gamma_3^2}{4\gamma_2} \quad \frac{D_3^2}{D_2} \tag{5.3}$$

The relation between D_3 and D_2 follows from the condition that the two jets must have the same strength at the nozzle, $U_0^2 \frac{\pi}{4} D_3^2 = U_0^2 D_2 L$, therefore

$$x_{tr} \sim \frac{\gamma_3^2}{\pi\gamma_2} L = 9.6\ L \tag{5.4}$$

The transition must occur downstream at a distance that scales with the nozzle width L but is one order of magnitude greater.

The numerical results presented in Figures 4.1 - 4.4 agree with these theoretical predictions. Specifically, the second change in Figure 4.1, the evolution of cross sectional shape for Re = 500, that corresponds to round cross-section, takes place around x/L = 10. This experimental result is in accord with the predicted result obtained from Eq. (5.4), namely $x_{tr}/L \sim 9.6$. Furthermore, Figure 4.2 shows that the evolution of turbulent jet flows at different Reynolds numbers follows the same pattern, and the transition lengths are virtually invariant throughout the Reynolds numbers. These results demonstrate the validity of Eq. (5.4), namely that the transition length of turbulent jet flows for different Reynolds numbers is a constant.

5.2. Laminar jets

The tendency to evolve from flat cross-sections to round cross-sections is also a characteristic of laminar jets, for which exact solutions exist in analytical form [21]. In the two-dimensional laminar jet the centerline velocity decreases as $x^{-1/3}$ in the downstream direction,

$$u_2 = 0.4543 \left(\frac{U_0^4 D_2^2 L^2}{\nu x} \right)^{1/3} \tag{5.5}$$

where D_2 and L are the dimensions of the slit. In the round jet issuing from a nozzle of diameter D_3, the centerline velocity decreases as x^{-1},

$$u_3 = \frac{3}{32} \frac{U_0^2 D_3^2}{\nu x} \tag{5.6}$$

The intersection of the two curves, Eqs. (5.5) and (5.6) yields the transition length

$$x_{tr,lam} = 0.132 \frac{U_0 D_3^2}{\nu}$$

$$= 0.168 L \frac{U_0 D_2}{\nu} \tag{5.7}$$

where we have used again the assumption that the two-dimensional jet has the same strength as the round jet.

The numerical results reported in Figures 3.1-3.6 support these theoretical predictions. Specifically, the first change in the curves of Figures 3.1-3.3 shows that the round cross-section is acquired roughly at x/L ~ 1.6, 3, and 4.8 for Re = 10, 20, and 30, respectively. These observations compare favorably with the results suggested by Eq.

(5.7), $x_{tr}/L \sim 1.68$, 3.36, and 5.04. To investigate a correlation between Reynolds number and transition length of laminar jets, the evolution of streamwise constant-velocity contours of Re = 10, 20, and 30 have been put together in Figure 3.4. It can be seen clearly that the change to the round cross section occurs farther from the nozzle when the Reynolds number is greater. Eq. (5.7) predicts correctly the relationship between Reynolds number and transition length.

6. Conclusions

In this paper we reported a theoretical and experimental study of rectangular laminar and turbulent jet flows. A computational model has been developed to simulate jets issuing from a rectangular nozzle. This part of our study was designed to observe the evolution of cross section of jet flows.

The laminar simulations show that the laminar jets of different Reynolds numbers have similar evolutionary patterns. The streamwise constant-velocity contours develop initially into shapes similar to the nozzle configuration and are followed by horizontal elliptical, circular, vertical elliptical, and circular contours again. The range of the transition length for laminar jets varies in direct proportion to nozzle exit velocity: laminar jet flows with higher Reynolds numbers acquire round cross-section farther downstream. The thesis further shows that turbulent jet flows with different Reynolds numbers become round at nearly the same downstream location.

In the theoretical part of this thesis, it is predicted that the transition length in laminar jet flow is proportional to Reynolds number and is constant in the case of turbulent jet. These predictions from constructal law are therefore reinforced by numerical results.

References

[1] A. Bejan, Advanced Engineering Thermodynamics. (2nd ed.), Wiley, Hoboken, 2006. [Bejan 1996, p. 815].

[2] A. Bejan. Constructal theory of pattern formation. Hydrol. Earth Syst. Sci. Discuss., 3, (2006) 1773–1807.

[3] L.B. Leopold, M.G. Wolman, and J. P. Miller, Fluvial Processes in Geomorphology, Freeman, San Francisco, 1964.

[4] R.C. Deo, J. Mi, G.J. Nathan, The Influence of Nozzle Aspect Ratio on Plane Jets, Experimental Thermal and Fluid Science, Vol.31, Issue 8, (Aug 2007) 825–838.

[5] R.S. Miller, C.K. Madnia, and P. Givi, Numerical simulation of non-circular jets, Computers & Fluids Vol. 24, No. 1 (1995) l-25.

[6] E.J. Gutmark, F.F. Grinstein, Flow Control With Noncircular, Annual Review of Fluid Mechanics (1999) 239-272.

[7] R. Wilson, Computations of complex Three-dimensional turbulent free jets, NASA-CR-201642, May 1997.

[8] J. J. McGuirk, W. Rodi, The Calculation of Three-Dimensional Turbulent Free Jets, Proceeding of the 1st Symposium on turbulent shear flows (university park, PA), (1977) 1.29-1.36.

[9] E. Gutmark, I. Wygnanski, The Planar Turbulent Jet, Journal of Fluid Mechanics , Vol.73, Issue 03 (1976) 465-495.

[10] G. Heskestad, Hot Wire Measurements in a Plane Turbulent Jet, Journal of Applied Mechanics, Vol.32 (1965) 721-734.

[11] K.W. Everittp, A.G. Robins, The Development and Structure of Turbulent Plane Jets, J. Fluid Mech.,vol. 88, part 3, (1978) 563-583.

[12] A.A. Sfeir, The Velocity and Temperature Fields of Rectangular Jets. International Journal of Heat and Mass Transfer, Vol.19 (1976) 1289-1383.

[13] N. Trentacoste, P. Sforza, Further Experimental Results for Three-Dimensional Free Jets. AIAA Journal Vol. 5, No. 5 (1967) 800-806.

[14] A.A. Sfeir, Investigation of Three-Dimensional Turbulent Rectangular Jets. AIAA journal, Vol.17 (1979) 1055-1060.

[15] P.M. Sforza, M.H. Steiger, and N. Trentacoste, Studies on Three-Dimensional Viscous Jets, AIAA Journal, Vol. 4 (1966) 800-806.

[16] G.N. Abramovich, The Theory of Turbulent Jets, MIT Press, Cambridge, MA., (1963).

[17] S.I. Pai, Fluid Mechanics of Jets, D. Van Nostrand Inc., Princeton, N. J. (1953).

[18] G.N. Abramovich, On the Deformation of the Rectangular Turbulent Jet Cross-Section. Int. J. Heat Mass Transfer, Vol.25, No. 12 (1982) 1885-1894.

[19] S.B. Pope, Turbulent Flows, Cambridge University Press, 2000.

[20] A. Bejan, S. Lorente, Why All Plumes And Jets Acquire Round Cross-sections, (December 2012), 8 pages, unpublished.

[21] A. Bejan, Convection Heat Transfer, 4th edition, Wiley, Hoboken (2013) chapter 9.